ISSN: 1410-8917
Jurnal Kimia Sains & Aplikasi
e-ISSN: 2597-9914

Jurnal Kimia Sains dan Aplikasi 24 (4) (2021): 126–135

Jurnal Kimia Sains dan Aplikasi
Journal of Scientific and Applied Chemistry

Journal homepage: http://ejournal.undip.ac.id/index.php/ksa

# Bandgap Energy of $TiO_2$/M-Chlorophyll Material (M=$Cu^{2+}$, $Fe^{3+}$)

Muhammad Yuspriyanto [a,b], Titin Anita Zaharah [a], Imelda Hotmarisi Silalahi [a,*]

[a] Department of Chemistry, Faculty of Mathematics and Natural Sciences, Tanjungpura University, Pontianak, Indonesia
[b] Industrial Research and Standardization Center, Pontianak, Indonesia

* corresponding author: imelda.h.silalahi@chemistry.untan.ac.id

https://doi.org/10.14710/jksa.24.4.126-135

Article Info

Article history:

Received: 9th March 2021
Revised: 18th April 2021
Accepted: 30th April 2021
Online: 30th April 2021

Keywords:
chlorophyll; $Cu^{2+}$-chlorophyll complex; $Fe^{3+}$-chlorophyll complex; Tauc plot method; bandgap energy

Abstract

The bandgap energy ($E_{gap}$) of $TiO_2$ material modified with metal-chlorophyll complex compounds (M = $Cu^{2+}$, $Fe^{3+}$) was observed. Chlorophyll (Chl) was isolated from cassava leaves, and its UV-Vis spectra showed absorption peaks in the Soret band region (410 nm) and in the Q band region (665 nm), which is the typical peak of chlorophyll. Copper(II)-chlorophyll complex was prepared from the reaction between chlorophyll and $CuSO_4.5H_2O$, while the iron(III)-chlorophyll was synthesized from chlorophyll and $FeCl_3.6H_2O$ in methanol solvent under reflux at 65°C. The presence of copper and iron metals in the chlorophyll metal complexes was identified using Atomic Absorption Spectroscopy in methanol solution. The absorption of copper measured in $Cu^{2+}$-Chl was 0.0488 (0.4805 mg/L), while the iron atom in $Fe^{3+}$-Chl was 0.0050 (0.0195 mg/L). The UV-vis spectra demonstrate the hypsochromic shift of the Soret band to 405 nm ($Cu^{2+}$-Chl) and 402 nm ($Fe^{3+}$-Chl). The Infrared spectra of chlorophyll after being complexed with copper(II) shows the increase of vibrational absorption wavenumber of the C=N group from 1225.06 $cm^{-1}$ to 1241.94 $cm^{-1}$ indicates the coordination of the metal ion on the N atom in the pyrrole ring. The shift in the absorption band on the $Fe^{3+}$-Chl spectrum was seen for the C=O ester group from 1720.49 $cm^{-1}$ to 1721.10 $cm^{-1}$ indicating the metal ion bonding in the C=O group of esters. The DR-UVis analysis of $TiO_2$/metal-chlorophyll shows a bathochromic shift towards the visible light region. By using the Tauc plot method, it was observed that the $E_{gap}$ of $TiO_2$ reduces from 3.08 eV to 2.89 eV and 2.93 eV in the compound of $TiO_2$/$Cu^{2+}$-Chl and $TiO_2$/$Fe^{3+}$-Chl, respectively.

## 1. Introduction

Material modification using complexes of transition metals and natural ligands such as chlorophyll, curcumin, and anthocyanins has been widely carried out. One of the uses of natural ligands is their use as a dye that functions as a photosensitizer that absorbs photon energy from sunlight in a solar cell system known as natural-Dye Sensitized Solar Cell (n-DSSC), as an alternative concept to conventional solar cells [1]. Previously, DSSCs were made using the poly-pyridyl ruthenium complex as an effective sensitizer. However, this material is not economical because of the low abundance of ruthenium metal, and it is not profitable from an environmental aspect. Another approach is to replace DSSC materials with complex compounds from abundant transition metals and natural dyes that are easy to extract, cost-efficient, environmentally friendly, non-toxic, readily available, and biodegradable.

As the primary pigment of photosynthesis, chlorophyll has a symmetric pyrrole ring that coordinates with the $Mg^{2+}$ ion in the central atom. Transition metals can potentially replace $Mg^{2+}$ ions to form metal-chlorophyll complexes [2]. There have been many observations on the luminosity of chlorophyll [3, 4, 5]. The luminescence property of chlorophyll is the basis for its use as a coloring agent in semiconductors.

Titanium(IV) oxide ($TiO_2$) is a semiconductor material used in DSSC. However, it has an immense bandgap energy (3.2 to 3.9 eV), so it only absorbs the ultraviolet portion of sunlight, giving it a relatively low conversion efficiency (5%) [6]. The efficiency can be

improved by increasing the absorption of sunlight by reducing the energy of the bandgap. The introduction or insertion of transition metals into $TiO_2$ material has been shown to reduce the bandgap energy. Copper oxide compounds are known to have low bandgap energies of 1.7 eV and 2.1 eV for CuO and $Cu_2O$, respectively [7]. The insertion of about 2% copper(II) metal ions in the $TiO_2$ structure without the occurrence of cation exchange has lowered the $E_{gap}$ of the material to 2.86 eV [8], while the doping of $TiO_2$ with Cu metal by up to 2.5%, which causes cation exchange reduces the bandgap energy to visible light [9]. Doping of $Fe^{3+}$ ion into $TiO_2$ to form $TiO_2/Fe_2O_3$ material shifts the valence band positively and has been reported to be photoactive in the photosynthetic reactions of methanol under visible light [10, 11, 12]. The combination of chlorophyll dye properties and the transition metal coordinated with the chlorophyll ligand incorporated with the $TiO_2$ material is expected to reduce the bandgap energy. This can widen the use of the material as a photocatalyst or sensitizer in DSSC.

In this study, chlorophyll was complexed with metal ions $Cu^{2+}$ and $Fe^{3+}$. The synthesized complex compound was then deposited on the $TiO_2$ surface. Characterization of complex compounds was carried out using a UV-Vis spectrophotometer, infrared spectrophotometer, and atomic absorption spectrophotometer. Meanwhile, $TiO_2$/metal-chlorophyll material was characterized by using Diffuse Reflectance (DR) UV-Vis. The Tauc plot method is used as the basis for calculating the bandgap energy value for $TiO_2/Cu^{2+}$-Chl and $TiO_2/Fe^{3+}$-Chl materials.

## 2. Methodology

### 2.1. Equipment and Materials

The equipment used was a separator funnel, furnace, hotplate, chromatography column, boiling flask, UV lamp, condenser, magnetic stirrer, rotary evaporator, a set of glassware, Perkin Elmer infrared spectrophotometer, Perkin Elmer atomic absorption spectrophotometer (AAS), UV-Visible spectrophotometer (UV-Vis) Shimadzu UV 2600, Shimadzu 2450 Diffuse Reflectance UV-Vis (DR/UV-Vis) spectrophotometer, and Mettler Toledo AE 60 analytical balance.

The materials used in this study were 99.7% glacial acetic acid (Merck), 99.8% acetonitrile (Merck), iron(III) chloride hexahydrate ($FeCl_3.6H_2O$), 99-102% (Merck), cassava leaves, dichloromethane 99.8% (Merck), ethanol 98% (Merck), ethyl acetate 99.75% (Merck), n-hexane 99% (Merck), all of which were analytical grade. In addition, 0.45 µm (Whatman) filter paper, fluorine tin oxide (FTO) conductive glass, methanol 99.8% (JTBaker), TLC plate silica gel 60 Å pore size, silica gel for column chromatography pore size 60 Å (Merck), copper(II) sulfate pentahydrate ($CuSO_4.5H_2O$) 99-100.5% (Merck) and titanium(IV) oxide ($TiO_2$) $P_{25}$ 99.5% nanopowder 21 nm (Aldrich) were used.

### 2.2. Chlorophyll isolation [13]

Cassava leaves (300 g) were crushed with a mortar with a bit of methanol added. An amount of 200 mL of methanol was added to the delicate leaves and then filtered. The residue was washed by using methanol three times. Then the methanol solutions were combined. The extraction was carried out using *n*-hexane as a solvent. 300 mL of *n*-hexane was added to the methanol solution, then placed in a separating funnel. Into the mixture, a saturated solution of NaCl (50 mL) was added. Then the top layer (*n*-hexane) was taken. The *n*-hexane solvent was evaporated by using a rotary evaporator to give a green solid. The extract was purified *via* silica in a chromatography column using the eluent *n*-hexane: ethyl acetate of 9: 1 to obtain chlorophyll.

### 2.3. Synthesis of copper(II)-chlorophyll complex [13]

In a 100 mL round bottom flask equipped with a condenser, 0.1 g (0.1 mmol) isolated chlorophyll was dissolved in 30 mL methanol. Copper sulfate pentahydrate ($CuSO_4.5H_2O$) (0.028 g, 0.1 mmol) was added to the chlorophyll solution while stirring. Then the mixture was refluxed for 4 hours at 65°C. The reaction was monitored by the thin-layer chromatography method at 0 minutes, 1 hour, 2 hours, 3 hours, and 4 hours using *n*-hexane: ethyl acetate of 9: 1 eluent. After that, the solvent was evaporated using a rotary evaporator. The complex compound formed was purified through the solvent extraction method in 10 mL dichloromethane washed three times with 10 mL distilled water. Furthermore, the dichloromethane solution was taken; then added anhydrous $MgSO_4$ to remove water. The filtrate was taken, and then the solvent was removed by using a rotary evaporator to give a light green solid. The product was characterized by using a UV-Vis spectrophotometer, atomic absorption spectrophotometer, and infrared spectrophotometer.

### 2.4. Synthesis of iron(III) - chlorophyll complexes [14]

In a 100 mL round bottom flask equipped with a condenser, 0.1 g (0.1 mmol) isolated chlorophyll was dissolved in 30 mL methanol. Then 0.030 g (0.1 mmol) of iron (III) chloride hexahydrate ($FeCl_3.6H_2O$) was added to the chlorophyll solution while stirring. The procedure was carried out to prepare the copper(II)-chlorophyll complex mentioned in section 2.3. The purification of complex compounds was carried out by using gravity column chromatography.

### 2.5. $TiO_2$ material preparation on conductive glass

$TiO_2$ paste was prepared in which 2 g of $TiO_2$ solid was crushed by using a mortar to obtain a fine solid. Acetic acid (5 mL) and ten drops of acetonitrile ($CH_3COCN$) were added and stirred using a magnetic stirrer to form a $TiO_2$ paste. The Fluorine Tin Oxide (FTO) conductive glass was cleaned by using ethanol. Then the $TiO_2$ paste was deposited on the active site of the FTO conductive glass with an area of 1 cm x 1 cm. The $TiO_2$ layer was left in the open air to dry then calcined in a furnace at 450°C for 2 hours.

### 2.6. $TiO_2$/metal chlorophyll material preparation

Chlorophyll complex solution was prepared at a concentration of 40 ppm by dissolving 2 mg of chlorophyll complex in 50 mL methanol. The adsorption process was carried out in which $TiO_2$ paste, which was

deposited on calcined FTO conductive glass, was immersed in 15 mL of chlorophyll complex solution. The immersion was carried out for 24 hours in the dark and closed. The absorbance of the solution was measured using a UV-Vis spectrophotometer before and after the adsorption to monitor the amount of compounds adsorbed by $TiO_2$.

### 2.7. Characterization of $TiO_2$/metal-chlorophyll material

The absorption of chlorophyll complex solution before and after adsorption on $TiO_2$ was measured using a UV-Vis spectrophotometer at a wavelength of 200-800 nm to determine the occurrence of adsorption. The characterization of $TiO_2$, $TiO_2$/metal-chlorophyll (M = $Cu^{2+}$ and $Fe^{3+}$) materials deposited on FTO conductive glass was carried out by using a Diffuse Reflectance UV-Vis (DR-UV-Vis) spectrophotometer, and the data obtained were analyzed by using the Tauc plot method to determine the change in bandgap energy ($E_{gap}$).

The $E_{gap}$ value was determined by using the Tauc Plot method in which a linear graph of photon energy, hν (eV) on the x-axis, and the coefficient, $(Khν)^2$ on the y-axis were drawn. The bandgap energy is the photon energy value from the x-axis intersection obtained from the regression equation [15, 16].

The Tauc plot equation is as follows:

$$(Khν)^{1/n} = K.E = \frac{(1-R)\hat{}2}{2R} \; \chi \; \frac{hc}{\lambda}$$

Note:
R = reflectance
h = Plank constant (6,626 x $10^{-34}$ J/s)
c = the speed of light (3 x $10^8$ m/s)
λ = wavelength (nm)
n = ½ (direct transition)

## 3. Results and Discussion

### 3.1. Chlorophyll Isolation and Characterization

Chlorophyll, which is used to synthesize metal-chlorophyll complex compounds, was isolated from cassava leaves using the extraction method. The thin-layer chromatography (TLC) results using *n*-hexane: ethyl acetate of 9: 1 eluent showed that spots based on the Retardation factor ($R_f$) value could be identified as the content of chlorophyll a, chlorophyll b, and β-carotene. Chlorophyll extract was separated through gravity column chromatography with an eluent mixture of *n*-hexane and ethyl acetate in a ratio of 9: 1. The β-carotene compounds, which are more non-polar, came out first, followed by chlorophyll to obtain β-carotene-free chlorophyll isolates. The chlorophyll isolate obtained was 1.7% of the number of cassava leaves used.

Chlorophyll electronic transition was observed in the UV-Vis spectra using methanol as a solvent. Methanol absorption is at a wavelength of 250-300 nm so that the absorption observed in this study is at a wavelength of > 300 nm. Figure 1 shows the chlorophyll absorption spectra obtained. Chlorophyll absorbs photons at a wavelength of 400-800 nm in two wavelength regions, namely the Soret band and the Q band. Several typical peaks of chlorophyll were obtained. This absorption peak was thought to result from an electronic transition $\pi \rightarrow \pi^*$ originating from the porphyrin ring found in two regions: the Soret band region and the Q band region. The isolated chlorophyll gave two prominent UV-Vis absorption peaks at 410 and 665 nm, accompanied by several weakly intense peaks at 509 nm, 543 nm, and 608 nm [14, 17]. The peak at 410 nm in the Soret band indicates a mixture of chlorophyll a and chlorophyll b. The four peaks in the Q band consisting of three peaks with weak intensity and one absorption peak in the 665 nm region have the most vigorous intensity. These absorption peaks originated from orbitals in the porphyrin structure which have four pyrrole rings. The absorption results indicate that chlorophyll can be used as a dye in DSSC because it shows absorption in the visible light region.

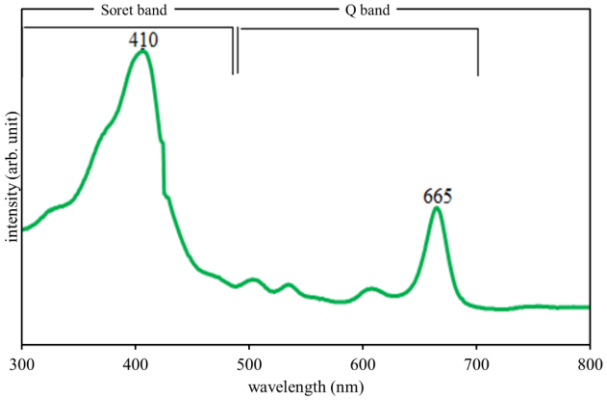


**Figure 1.** UV-Vis chlorophyll (Chl) spectra in methanol solvent.

Characterization of isolated chlorophyll using an infrared spectrophotometer showed a bending vibration of the N-H group at a wavenumber of 1627.22 $cm^{-1}$. The broad and robust peak at 3379.75 $cm^{-1}$ is an OH group that may come from a water molecule interacting with the C=O group from the ester and keto groups. The OH peak can also be due to the enolization of β-hydrogen in the keto ring, in which the keto group in chlorophyll is a diastereoisomeric compound [13]. The bending vibration of the CN group on the pyrrole group occurred at 1225.06 $cm^{-1}$, corresponding to the porphyrin peak reported in a previous study [18]. The hydrocarbon group, C-H in the phytol chain, is shown at wave number 2923.97 $cm^{-1}$. A strong peak at 1720.49 $cm^{-1}$ indicates a vibrational C=O ester group, while a peak at wave number 1450.50 $cm^{-1}$ indicates a C=C functional group.

### 3.2. Synthesis and Characterization of Copper(II) - Chlorophyll Complexes ($Cu^{2+}$-Chl)

The $Cu^{2+}$-Chl complex was prepared from the reaction of the $CuSO_4.5H_2O$ compound, the precursor for the $Cu^{2+}$ ion, with the chlorophyll as a ligand. The reaction is carried out in the form of a solution using methanol as a solvent because methanol is a solvent capable of dissolving chlorophyll and $CuSO_4.5H_2O$ well [2]. The two compounds are put into a boiling flask equipped with a condenser, magnetic stirrer and placed on an electric heater. The reaction was conducted under the reflux condition for 4 (four) hours, followed by TLC to observe

the reaction with time variations of 0 minutes (before reflux), 2 hours, and 4 hours. TLC results at 0 minutes showed that there were three spots identified as chlorophyll a, chlorophyll b, and pheophytin a. At the reflux time of 2 hours, no chlorophyll and pheophytin a spots appeared, but a new spot with an $R_f$ value of 0.60 was observed, which was identified as the product of the reaction. At the reaction time of 4 hours, the $R_f$ shifted slightly from the initial spot of the product to 0.70 with a single spot; the solution color change to a lighter green, indicating the formation of the reaction product, $Cu^{2+}$-Chl compound.

To identify copper (Cu) metal in the product, analysis was made using atomic absorption spectrophotometry. The test begins with the preparation of a metal ion calibration curve by making a standard series through the dilution of Certified Reference Material (CRM) from Mg and Cu metals from a concentration of 1000 mg/L to several working standards in the concentration range of 0-0.1 mg/L (Mg) and 0-5 mg/L (Cu). Metal absorbances were measured at the wavelengths of 285.2 nm (Mg) and 324.8 nm (Cu) until a straight-line equation was obtained with a linear regression correlation coefficient ($R^2$) ≥ 0.995. Sample preparation was carried out by dissolving solid chlorophyll and $Cu^{2+}$-Chl complex in methanol with a concentration of 20-30 mg/L in a 100 mL volumetric flask. The test samples were then filtered through a 0.45 µm membrane then the absorbance of metal ions in the test samples along with the solvent blank was measured on AAS at a wavelength of 285.2 nm (Mg) and 324.8 nm (Cu). The measurements for a solution of chlorophyll in methanol showed that Mg metal absorbance was 0.0827 (C = 0.0952 mg/L), while, the measurement of Cu metal showed zero Cu uptakes. This result is in accordance with the structure of chlorophyll, which has Mg as the central atom. Measurement of $Cu^{2+}$-Chl complex solution in methanol showed that Cu uptake was 0.0488 (C = 0.4805 mg/L) and Mg metal uptake decreased compared to chlorophyll to 0.0518 (C = 0.0482 mg/L). Metal concentration was obtained by comparing the absorbance of metal ions with a calibration curve with linear regression values $R^2$ = 0.9964 (Mg metal) and 0.9985 (Cu metal) (Figure 2). The presence of Cu uptake and decreased Mg uptake in the $Cu^{2+}$-Chl complex solution indicates the presence of metal in the complex compound but cannot prove that metal complexation or the substitution of the central atom in chlorophyll has occurred.

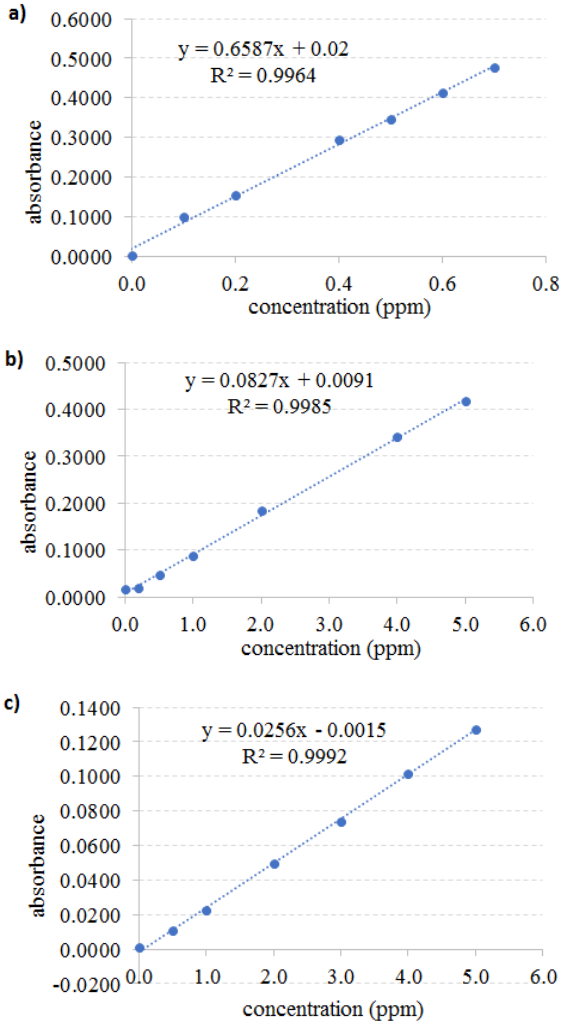


**Figure 2.** Atomic absorption calibration curves using AAS for a) Mg (λ=285.2 nm), b) Cu (λ=324.8 nm) and c) Fe (λ=248.3 nm)

UV-Vis spectrophotometer was used to study the electronic transition of $Cu^{2+}$-Chl complexes compared to chlorophyll. The spectra depicted in Figure 3 show consistency with the results of previous studies [14, 19]. Chlorophyll spectra show peaks in the Soret band with a maximum wavelength of 410 nm, while the visible light region is at 665 nm. Changes are seen in the spectra of complex compounds where new peaks appear at a wavelength of 405 nm. There is a hypsochromic shift or blue shift at the peak of 410 nm to 405 nm. A wavelength shift also occurs in the visible region, a hypsochromic shift from 665 nm to 651 nm. The entry of copper(II) transition metals resulted in a significant increase in absorption intensity (hyperchromic effect) in chlorophyll metal complexes. The peak shift indicated the exchange of the central atom of the $Mg^{2+}$ ion in chlorophyll with the transition metal ion [2].

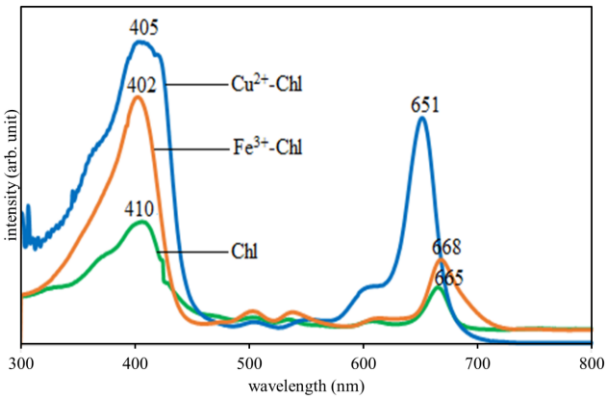


**Figure 3.** UV-vis spectra of $Fe^{3+}$-Chl and $Cu^{2+}$-Chl compounds compared to Chl

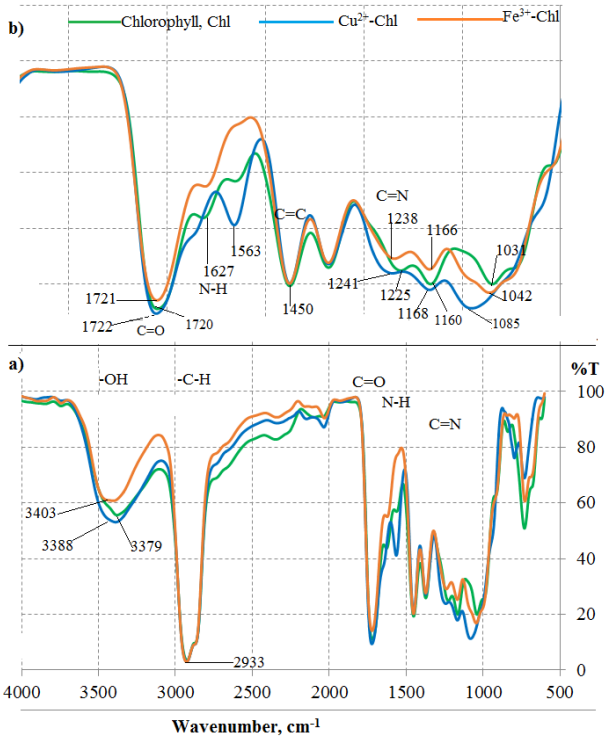


Figure 4. Infrared spectra of (a) Chlorophyll (Chl) (green line), $Cu^{2+}$-Chl (blue line) and $Fe^{3+}$-Chl (orange line), (b) enlarged spectra in the area 1000-2000 $cm^{-1}$ to make more detail

The FT-IR spectra of the $Cu^{2+}$-Chl complex compound compared to chlorophyll (Figure 4) show that the vibrational energy associated with the O-H functional group shifted to a higher wavenumber 3379.75 $cm^{-1}$ to 3388.75 $cm^{-1}$. The shift in wavenumbers indicates a change in the enol group due to the interaction of water molecules with the metal. The appearance of this OH group can be derived from the enolization of beta-hydrogen in the keto ring. The keto group in chlorophyll is a diastereoisomeric compound that can facilitate keto-enol tautomerism [13]. An insignificant shift was observed in the C=O ester functional group (from the five-membered ring in the chlorophyll structure), from 1720.49 $cm^{-1}$ to 1722.63 $cm^{-1}$. The change in the vibration band in C=O ester is influenced by the entry of $Cu^{2+}$ ions into the chlorophyll, thereby increasing the vibration absorption in the C=O ester group [13]. The absorption peak for the N-H group in chlorophyll at 1627.22 $cm^{-1}$ did not appear in the $Cu^{2+}$-chlorophyll spectra. The associated peak for the C=N group has shifted from 1225.06 $cm^{-1}$ to 1241.94 $cm^{-1}$, indicating the possibility that the $Cu^{2+}$ ion is coordinated with the N atom in the pyrrole ring, replacing the $Mg^{2+}$ ion. Although the shift in wavenumbers in the IR spectra is insufficient to prove the structure of a complex compound, the observed trends indicate the coordination of $Cu^{2+}$ ions with N atoms in the pyrrole system.

**Table 1.** Annotation of Functional Groups in $Cu^{2+}$-Chl and $Fe^{3+}$-Chl Compounds compared to Chl based on FTIR Spectra

| Chl ν ($cm^{-1}$) | $Cu^{2+}$-Chl ν ($cm^{-1}$) | $Fe^{3+}$-Chl ν ($cm^{-1}$) | Functional group | References [14] |
|---|---|---|---|---|
| 3379.75 | 3388.75 | 3403.18 | O-H | 3800 - 2700 |
| 2923.97 | 2925.90 | 2927.45 | C-H | 3000 - 2850 |
| 1720.49 | 1722.63 | 1721.10 | C=O | 1850 -1600 |
| 1627.22 | -- | 1620.55 | N-H | 1640 - 1550 |
| 1225.06 | 1241.94 | 1238.45 | C=N | 1250 - 1000 |
| 1450.50 | 1451.04 | 1451.52 | C=C | 1900 - 1400 |

ν = wavenumber

### 3.3. Synthesis and Characterization of Iron(III)-Chlorophyll ($Fe^{3+}$-Chl) Complexes

The synthesis of $Fe^{3+}$-Chl complexes was carried out using $FeCl_3.6H_2O$ compound as a precursor for $Fe^{3+}$ metal ion, which was reacted with chlorophyll. At 0 min, when the precursor and chlorophyll were mixed, the TLC results showed a spot at $R_f$ 0.5, which was identified as chlorophyll. At the reflux time of 2 hours, the $R_f$ value for chlorophyll compound at $R_f$ 0.5 and several new spots at $R_f$ 0.75 and 0.87 were seen. At the reaction time of 4 hours, the chlorophyll spot was still observed at $R_f$ 0.5, while the additional spots shifted slightly to 0.75 and 0.95. The results of the TLC analysis showed that the reaction mixture still contained chlorophyll after 4 hours of reflux. So, it is necessary to purify the reaction product by gravity column chromatography using silica gel to obtain a single spot. The separation using the column showed a single spot identified as a complex compound product with an $R_f$ of 0.95 and intense green color.

AAS analysis was carried out to identify the presence of Mg and Fe metals in the $Fe^{3+}$-Chl complex compared to chlorophyll. AAS analysis was performed with the same treatment as $Cu^{2+}$-Chl measurements. The calibration curve is made from a standard series through the dilution of the Certified Reference Material (CRM) for Mg and Fe from a concentration of 1000 mg/L to several working standards in the concentration range of 0-0.1 mg/L (Mg) and 0-5 mg/L (Fe). The absorbance of metal ions was measured at 285.2 nm (Mg) and 248.3 nm (Fe). Sample preparation was carried out by dissolving chlorophyll solids and the $Fe^{3+}$-Chl complex into methanol with a 20-30 mg/L concentration in a 100 mL volumetric flask. The test samples were filtered using a 0.45 µm membrane, then the absorbance of metal ions in the test samples and solvent blank were measured using AAS at a wavelength of 285.2 nm (Mg) and 248.3 nm (Fe). The measurement results of the $Fe^{3+}$-Chl complex solution in methanol showed that the absorbance of Fe atoms was 0.005 and the absorption of Mg atoms decreased compared to

chlorophyll from 0.0827 to 0.0422. The metal ion concentration was obtained by comparing the absorbance of metal ions with a calibration curve with a linear regression value ($R^2$) of 0.9964 (Mg metal) and 0.9992 (Fe metal) (Figure 2) in order to obtain a Fe concentration of 0.0195 mg/L and Mg decreased from 0.0952 mg/L to 0.0337 mg/L. The adsorption of Fe metal indicates $Fe^{3+}$ ions in the $Fe^{3+}$-Chl compound, although it cannot prove the complexation between $Fe^{3+}$ and chlorophyll.

The results of the characterization of the complex $Fe^{3+}$-Chl compound using a UV-Vis spectrophotometer showed spectra changes in the Soret band area, where a new peak appeared at a wavelength of 402 nm (Figure 3). The peak shift from 411 nm to 402 nm is a hypochromic or blue shift to shorter wavelengths. The peak shift indicates that there has been a reaction to the formation of the $Fe^{3+}$-chlorophyll complex. It is estimated that an electronic transition factor influences the shift in wavelength in Metal-to-Ligand Charge Transfer (MLCT), the transition of electrons from metals to ligands [20]. The d-d transition can influence the MLCT phenomenon and the maximum wavelength in the visible light area. So that $Fe^{3+}$-chlorophyll can be used as a dye in DSSC because it can absorb light optimally. Meanwhile, in the Q band, there is a shift in wavelength to a higher direction (redshift), from 665 nm to 668 nm. The redshift can occur due to the complexation of chlorophyll with the $Fe^{3+}$ ion, which gives the auxochrome effect. Auxochrome compounds and solvents with a lower degree of polarity cause a redshift in the dye [21].

The characterization of $Fe^{3+}$-Chl complex compounds using infrared spectrophotometer shows the spectra shown in Figure 4, while the functional group annotations compared to chlorophyll are tabulated in Table 1. The vibrational energy associated with the -OH group experienced a shift at a higher wavenumber, 3403.18 $cm^{-1}$, compared to the chlorophyll spectra of 3379.75 $cm^{-1}$. The same trend was observed in the $Cu^{2+}$-Chl complex, which indicated a change in the enol group or the interaction of water molecules with the metal. The shifting of the vibrational band was also observed for the C=O ester group, showing a slight increase, from 1720.49 $cm^{-1}$ to 1721.10 $cm^{-1}$. Meanwhile, the peak associated with the C=N group increased from 1225.06 $cm^{-1}$ to 1238.45 $cm^{-1}$. The information obtained from the IR spectra of the $Fe^{3+}$-Chl compound did not seem to be sufficient to prove the formation of the $Fe^{3+}$-Chl complex. However, the TLC results and changes in wavelength in the UV-vis spectra indicated the formation of the complex.

Based on the data that has been described and the reaction products that have been discussed, it can be predicted that the complexation reaction of $Cu^{2+}$ ions with chlorophyll can be predicted as follows:

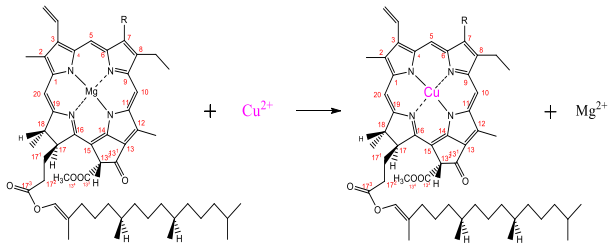


**Figure 5.** Prediction of the complexation reaction of $Cu^{2+}$ ions with chlorophyll to form $Cu^{2+}$-Chl

According to the Lewis acid-base concept, an acid is a species that accepts an electron pair, and a base is a species that donates an electron pair. Hard acids and bases are generally described in ionic interactions, whereas soft acids and bases are more covalent. Hard acids tend to bind to hard bases, and soft acids bind to soft bases [22]. Judging from the strength of the acid, in the theory of HSAB (Hard Soft Acid Base), $Cu^{2+}$ ions as borderline metal ions will like borderline donor atoms such as N in porphyrin. The $Cu^{2+}$ ion has the potential to substitute $Mg^{2+}$ in porphyrins so that $Cu^{2+}$ ions will replace the position of $Mg^{2+}$ as the center atom in the porphyrin ring in the chlorophyll structure. This prediction was supported by the results of the IR spectra on the $Cu^{2+}$-Chl complex compounds in which there was a significant shift in the absorption peak of the N-H groups, indicating the coordination of $Cu^{2+}$ ions in the N groups of chlorophyll.

The substitution of the metal ion $Mg^{2+}$ by $Cu^{2+}$ can also be considered based on the chemical properties of the metal element. Mg metal is electropositive, while Cu metal has a relatively high electronegativity of 1.90 on the Pauling scale [23]. The electronegativity possessed by $Cu^{2+}$ ions causes $Cu^{2+}$ metal to prefer coordinating with N atoms to make it easier to react.

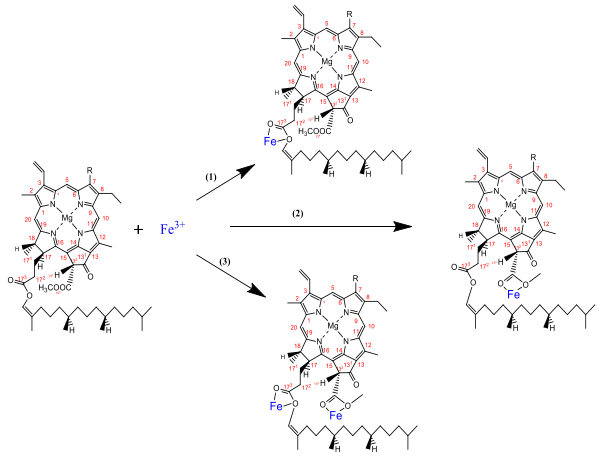


**Figure 6.** Prediction of the complexation reaction of $Fe^{3+}$ ion with chlorophyll to form $Fe^{3+}$-Chl

Figure 6 shows the prediction of the complexation reaction of metal ion $Fe^{3+}$ with chlorophyll. The $Fe^{3+}$ ion has a different behavior from the $Cu^{2+}$ ion. Based on the HSAB theory, the metal ion $Fe^{3+}$ is a hard acid, so it will prefer the $COO^-$ group, which is a hard base. The $Fe^{3+}$ ion bond can be coordinated selectively in either $COO^-$ or both. The structure of the $Fe^{3+}$-chlorophyll ion complex compound has 3 (three) possibilities according to the

reaction because the IR spectra results cannot prove that the reaction product is more dominant to either one.

### 3.4. Synthesis of $TiO_2$/Metal-Chlorophyll Materials

Titanium dioxide, which was sensitized on FTO glass, was prepared in the form of $TiO_2$ paste. The paste was made by adding 5 mL of acetic acid ($CH_3COOH$) and ten drops of acetonitrile ($CH_3COCN$) to 2 g of solid $TiO_2$. The addition of acetic acid aims to provide an acidic atmosphere to $TiO_2$, while acetonitrile functions as a particle stabilizer to prevent particle reaggregation. Stirring was carried out using a magnetic stirrer to form a $TiO_2$ paste. $TiO_2$ is made in the form of a paste (gel phase) because the gel phase can keep moving electrons well and provide a long-wear resistance. After all, it does not evaporate quickly. In making $TiO_2$ paste, the ratio of the amount of $TiO_2$ to liquid material (acetic acid and acetonitrile) must be considered because if the ratio of $TiO_2$/liquid material is too high, the resulting $TiO_2$ paste is too thick and can make the thin layer of $TiO_2$ too thick, making it easily peeled off the glass surface of the FTO. On the other hand, if the ratio of $TiO_2$/liquid material is too low, the $TiO_2$ paste is too liquid and can make the layer too thin, resulting in an easily volatile layer and not strong enough to absorb photons [24].

The $TiO_2$ paste is then positioned on the active site of the Fluorine Tin Oxide (FTO) conductive glass. The FTO glass is used because FTO glass is a conductive transparent glass that can carry loads to function as a cargo transport medium. The $TiO_2$ paste layer deposited on the FTO glass was then calcined at 450°C for 2 hours [25]. The purpose of calcination is to remove solvent molecules and rearrange the $TiO_2$ crystal structure so that the $TiO_2$ surface becomes homogeneous and forms pores with a large area. Choosing a moderately high calcination temperature needs to be considered to prevent agglomeration, which results in an increase in particle size and a decrease in the active surface area. Listanti *et al.* [26] reported that agglomeration occurred during the calcination of $TiO_2$ at 600°C.

**Table 2.** The UV-Vis Absorbance of $Cu^{2+}$-chlorophyll and $Fe^{3+}$-chlorophyll Solutions in Methanol, Before and After the Adsorption on $TiO_2$ Layer

| Complexes | λ (nm) | Absorbance | | |
|---|---|---|---|---|
| | | before adsorption | after adsorption | % adsorbed |
| $Cu^{2+}$-Chl | 405 | 0.908 | 0.885 | 2.53% |
| $Fe^{3+}$-Chl | 402 | 0.882 | 0.870 | 1.36% |

The adsorption process was carried out by immersing $TiO_2$-sensitized FTO glass in chlorophyll solution and M-chlorophyll complex solution (M = $Cu^{2+}$ and $Fe^{3+}$) under dark conditions for 24 hours. The immersion time was 24 hours as the optimum time for adsorption, affects the concentration of dye molecules adsorbed on the $TiO_2$ layer [27]. Another thing that affects the adsorption is the size of the $TiO_2$ particles. The smaller the $TiO_2$ particle size, the more dye will be adsorbed on the $TiO_2$ surface, providing a greater chance of photon absorption, increases the number of electrons injected into the $TiO_2$ particle [28]. The UV-Vis spectra of the chlorophyll complex solution showed a decrease in absorbance after the adsorption process, as shown in Table 2.

### 3.5. Band Gap Energy ($E_{gap}$) of $TiO_2$/Metal-Chlorophyll (M = $Cu^{2+}$, $Fe^{3+}$)

The $TiO_2$/metal-chlorophyll ($TiO_2$/M-Chl) materials were characterized using a Diffuse Reflectance UV-Vis (DR/UV-Vis) spectrophotometer analyze the UV-Vis reflectance characteristics and calculate the bandgap energy of the material. The DR/UV-Vis spectra of the synthetic materials were then compared with $TiO_2$.

The bandgap energy affects the electron excitation process from the valence band to the conduction band and the performance of a semiconductor as a photocatalyst material. When a semiconductor is subjected to photon energy, the electrons are excited to the conduction band, leaving a positive charge called a hole. Most of these electron-hole pairs will survive on the semiconductor surface so that the holes can work by initiating oxidation reactions. In contrast, the electrons initiate the reduction reactions of chemical compounds around the $TiO_2$ surface. If the bandgap energy is small, the light energy required is also tiny.

The determination of the bandgap energy value using the Tauc plot method is done by extrapolating the linear region from the relationship graph of hν with $(Kh\nu)^2$ so that it intersects the axis at y = 0. The hν value of the horizontal axis at y = 0 is the bandgap energy ($E_{gap}$). The scatter diagram of hν against $(Kh\nu)^2$ resulted from the DR-UV-Vis measurement for pure $TiO_2$ material at a 200-800 nm wavelength gives a linear line equation y = 3.1959x-9.8362 with y = 0 ( Figure 7a). Based on this equation, the $E_{gap}$ of $TiO_2$ is 3.08 eV, corresponding to a wavelength of 403 nm. The bandgap energy of undoped $TiO_2$ was previously reported in the range of 3.0-3.1 eV [29, 30].

A semiconductor doped with an element that contains an excess of electrons will generate donor energy so that the energy required for electrons to move from the valence band to the conduction band (bandgap) decreases. Dyes that can be used as sensitizers are adsorbable dyes with functional groups that can chemically bond to the $TiO_2$ surface and have a suitable energy level for electron injection. When the photons hit the electrodes on the DSSC, the energy of these photons is absorbed by the dye solution attached to the $TiO_2$ particles so that the electrons get the energy to be excited (dye*). The excited electrons are then injected into the $TiO_2$ conduction band, which acts as an electron acceptor/collector.

Based on calculations using the Tauc plot method, it was obtained the line equation y = 6.5724x-19.017 with a regression coefficient of 0.9906 for the $TiO_2/Cu^{2+}$-Chl material (Figure 7b). Through this equation, an $E_{gap}$ of 2.89 eV is obtained with a wavelength of 429 nm. This shows a decrease in bandgap energy when compared to $TiO_2$. This is similar to the previously reported value of Cu-doped-$TiO_2$ of 2.86 eV [8]. The success of the $Cu^{2+}$-Chl dye in $TiO_2$ sensitization can be seen from the

bathochromic shift (redshift) that occurs in the visible light region, from a wavelength of 403 nm ($TiO_2$) to 429 nm ($TiO_2$/$Cu^{2+}$-Chl). Adsorption of $Cu^{2+}$-Chl complex compounds by $TiO_2$ causes an interaction between $TiO_2$ and $Cu^{2+}$-Chl as a sensitizer. Electron clouds of metal ions fill the empty bands in $TiO_2$. The bathochromic shift indicates the interaction of $Cu^{2+}$ metal with $TiO_2$, caused by the injection of electrons from the excited state of the $Cu^{2+}$-Chl complex compound to the $TiO_2$ conduction band.

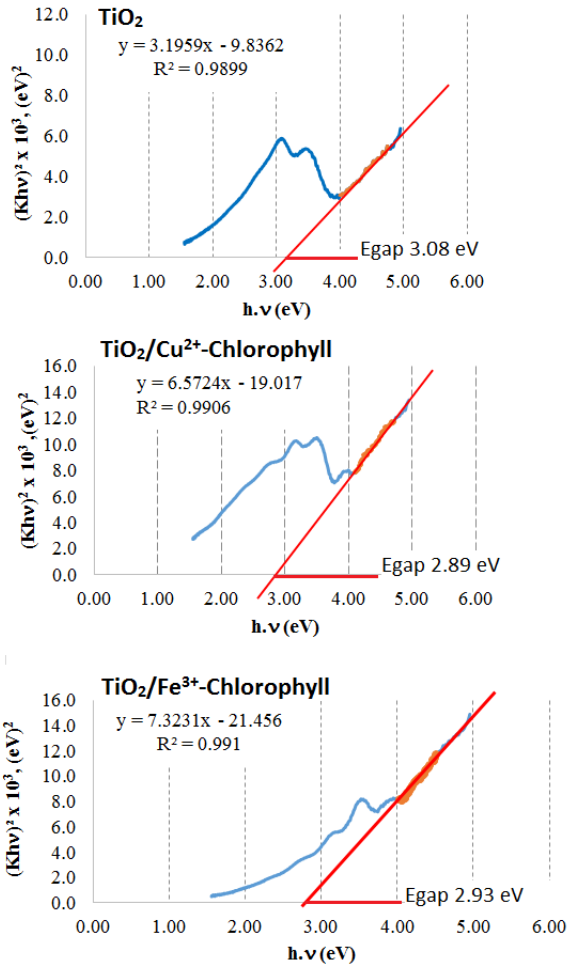


**Figure 7.** The modified reflectance spectra of the material based on the Tauc plot method for (a) $TiO_2$, (b) $TiO_2$/$Cu^{2+}$-Chl, (c) $TiO_2$/$Fe^{3+}$-Chl

Measurement of absorption and reflectance value (%R) using a DRUV/Vis spectrophotometer was also done on the $TiO_2$/$Fe^{3+}$-Chl material. Figure 7c shows the $TiO_2$ spectra sensitized by the $Fe^{3+}$-Chl complex. The measurement gave the line equation y = 7.3231x-21.456 with a regression coefficient of 0.9910. The Tauc plot method calculation results in the $E_{gap}$ value of 2.93 eV associated with a wavelength of 423 nm. The result shows the same tendency with $TiO_2$/$Cu^{2+}$-Chl material, in which there is a redshift (bathochromic) compared to the pure $TiO_2$ wavelength from 403 nm to 423 nm in $TiO_2$/$Fe^{3+}$-chlorophyll. This shift causes a decrease in the bandgap energy of the $TiO_2$ semiconductor to 2.93 eV. This reduction was smaller than the values reported for the Fe-doped $TiO_2$ material [10, 11], probably due to the relatively lower amount of $Fe^{3+}$-Chl material adsorbed in $TiO_2$. Increasing the concentration of dopant metal in doped-$TiO_2$ in the range of 1.0% to 2.0% causes a decrease in the material $E_{gap}$ [8]. Based on the measurement data and calculations using the Tauc plot method described above, the wavelength values and bandgap energy values of the $TiO_2$/metal-chlorophyll material are presented in Table 3.

**Table 3.** Value of wavelength (λ) and bandgap energy of $TiO_2$/M-Chl material

| Compound or complexes | λ (nm) | $E_{gap}$ (eV) |
|---|---|---|
| $TiO_2$ | 403 | 3.08 |
| $TiO_2$/$Cu^{2+}$-Chl | 429 | 2.89 |
| $TiO_2$/$Fe^{3+}$-Chl | 423 | 2.93 |

## 4. Conclusion

Based on the research results, it can be concluded that the bandgap energy ($E_{gap}$) of $TiO_2$ material sensitized by the chlorophyll metal complex compounds (M = $Cu^{2+}$, $Fe^{3+}$) reduces towards the lower energy compared to the pure $TiO_2$ material. The $E_{gap}$ of the materials is calculated using the Tauc plot equation based on diffuse reflectance data measured in the DR/UV-Vis spectrophotometer. The calculated $E_{gap}$ of the $TiO_2$/$Cu^{2+}$- chlorophyll is 2.89 eV (429 nm), and the bandgap energy of the $TiO_2$/$Fe^{3+}$-chlorophyll is 2.93 eV (423 nm), lower than that of the $TiO_2$ material, i.e., 3.08 eV (403 nm). The reduction of $E_{gap}$ in metal-chlorophyll-sensitized-$TiO_2$ materials (M = $Cu^{2+}$, $Fe^{3+}$) can increase the use of $TiO_2$ semiconductors.

## References

[1] Michael Grätzel, Dye-sensitized solar cells, *Journal of Photochemistry and Photobiology C: Photochemistry Reviews*, 4, 2, (2003), 145-153 https://doi.org/10.1016/S1389-5567(03)00026-1

[2] Jelena Petrovic, Goran Nikolic, Dejan Markovic, In vitro complexes of copper and zinc with chlorophyll, *Journal of the Serbian Chemical Society*, 71, 5, (2006), 501-512 http://dx.doi.org/10.2298/JSC0605501P

[3] Sergey V. Gaponenko, Pierre-Michel Adam, Dmitry V. Guzatov, Alina O. Muravitskaya, Possible nanoantenna control of chlorophyll dynamics for bioinspired photovoltaics, *Scientific Reports*, 9, 1, (2019), 7138 https://doi.org/10.1038/s41598-019-43545-4

[4] Zainal Arifin, Sudjito Soeparman, Denny Widhiyanuriyawan, Suyitno Suyitno, Argatya Tara Setyaji, Improving Stability of Chlorophyll as Natural Dye for Dye-Sensitized Solar Cells, *Jurnal Teknologi*, 80, 1, (2017), 27-33 https://doi.org/10.11113/jt.v80.10258

[5] M. Ridwan, E. Noor, Mohd Shahrizal Rusli, Akhiruddin, Fabrication of dye-sensitized solar cell using chlorophylls pigment from sargassum, *IOP Conference Series: Earth and Environmental Science*, 144, (2018), 012039 https://doi.org/10.1088/1755-1315/144/1/012039

[6] Brian O'Regan, Michael Gratzel, A low-cost, high-efficiency solar cell based on dye-sensitized colloidal $TiO_2$ films, *Nature*, 353, 6346, (1991), 737-740 https://doi.org/10.1038/353737a0

[7] Xiliang Nie, Su-Huai Wei, S. B. Zhang, First-principles study of transparent p-type conductive $SrCu_2O_2$ and related compounds, *Physical Review B*,

65, 7, (2002), 075111
https://doi.org/10.1103/PhysRevB.65.075111

[8] Gladis Pedroza-Herrera, Iliana E. Medina-Ramírez, Juan Antonio Lozano-Álvarez, Sandra E. Rodil, Evaluation of the Photocatalytic Activity of Copper Doped $TiO_2$ nanoparticles for the Purification and/or Disinfection of Industrial Effluents, *Catalysis Today*, 341, (2020), 37-48
https://doi.org/10.1016/j.cattod.2018.09.017

[9] Trang Nguyen Thi Thu, Nhiem Nguyen Thi, Vinh Tran Quang, Khanh Nguyen Hong, Tan Nguyen Minh, Nam Le Thi Hoai, Synthesis, characterisation, and effect of pH on degradation of dyes of copper-doped $TiO_2$, *Journal of Experimental Nanoscience*, 11, 3, (2016), 226-238
https://doi.org/10.1080/17458080.2015.1053541

[10] Amir Abidov, Bunyod Allabergenov, Oybek Tursunkulov, Lili He, Beom-Hyeok Park, Hee-Joon Kim, Sungjin Kim, Methanol Artificial Photosynthesis Using Iron Doped $TiO_2$, *Journal of Biobased Materials and Bioenergy*, 8, 2, (2014), 165-169 https://doi.org/10.1166/jbmb.2014.1429

[11] Amir Abidov, Bunyod Allabergenov, Jeonghwan Lee, Heung-Woo Jeon, Soon-Wook Jeong, Sungjin Kim, X-Ray Photoelectron Spectroscopy Characterization of Fe Doped $TiO_2$ Photocatalyst, *International Journal of Materials, Mechanics and Manufacturing*, 1, (2013), 294-296 https://doi.org/10.7763/ijmmm.2013.v1.63

[12] Rita Prasetyowati, Laila Katriani, Yunita Ambarwati, Studi Preparasi dan Karakterisasi Sel Surya Berbasis Titania Melalui Penyisipan Logam Tembaga (Cu) dengan Berbagai Variasi Massa pada Lapisan Aktif Titania, *Jurnal Sains Dasar*, 6, 1, (2017), 1-7
https://doi.org/10.21831/jsd.v6i1.12129

[13] Imelda Hotmarisi Silalahi, Julan Julan, Muhammad Yusprianto, Rudiyansyah Rudiyansyah, Sintesis dan Transisi Elektronik Kompleks Tembaga(II)-Klorofil, *Indonesian Journal of Pure and Applied Chemistry*, 3, 3, (2020), 1-9

[14] Roberta Anjelia, Imelda Hotmarisi Silalahi, Gusrizal Gusrizal, Sintesis dan Transisi Elektronik Senyawa Kompleks Klorofil dengan Logam (M = $Co^{2+}$, $Fe^{3+}$), *Indonesian Journal of Pure and Applied Chemistry*, 2, 3, (2019), 102-111

[15] Jonathan P. Blitz, Diffuse Reflectance Spectroscopy, in: F.M. Mirabella (Ed.) *Modern Techniques in Applied Molecular Spectroscopy*, John Wiley & Sons, Inc, New York, 1998

[16] Patrycja Makuła, Michał Pacia, Wojciech Macyk, How To Correctly Determine the Band Gap Energy of Modified Semiconductor Photocatalysts Based on UV–Vis Spectra, *The Journal of Physical Chemistry Letters*, 9, 23, (2018), 6814-6817
https://doi.org/10.1021/acs.jpclett.8b02892

[17] Aziza Hfii Ahliha, Fahru Nurosyid, Agus Supriyanto, Triana Kusumaningsih, The chemical bonds effect of anthocyanin and chlorophyll dyes on $TiO_2$ for dye-sensitized solar cell (DSSC), *Journal of Physics: Conference Series*, 909, (2017), 012013
https://doi.org/10.1088/1742-6596/909/1/012013

[18] C. S. Clemente, V. G. P. Ribeiro, J. E. A. Sousa, F. J. N. Maia, A. C. H. Barreto, N. F. Andrade, J. C. Denardin, G. Mele, L. Carbone, S. E. Mazzetto, P. B. A. Fechine, Porphyrin synthesized from cashew nut shell liquid as part of a novel superparamagnetic fluorescence nanosystem, *Journal of Nanoparticle Research*, 15, 6, (2013), 1739
https://doi.org/10.1007/s11051-013-1739-6

[19] Martin Gouterman, Georges H. Wagnière, Lawrence C. Snyder, Spectra of porphyrins: Part II. Four orbital model, *Journal of Molecular Spectroscopy*, 11, 1, (1963), 108-127
https://doi.org/10.1016/0022-2852(63)90011-0

[20] Harsasi Setyawati, Handoko Darmokoesoemo, Anggy Tamara Ayu Ningtyas, Yassine Kadmi, Hicham Elmsellem, Heri Septya Kusuma, Effect of metal ion Fe(III) on the performance of chlorophyll as photosensitizers on dye sensitized solar cell, *Results in Physics*, 7, (2017), 2907-2918
https://doi.org/10.1016/j.rinp.2017.08.009

[21] Aziza Hfii Ahliha, Fahru Nurosyid, Agus Supriyanto, Kajian pH Klorofil Terhadap Ikatan Kimia Dye pada $TiO_2$ sebagai Aplikasi Dye-Sensitized Solar Cell (DSSC), *Jurnal Fisika dan Aplikasinya*, 14, 1, (2018), 16-19
https://dx.doi.org/10.12962/j24604682.v14i1.3163

[22] Ralph G. Pearson, Hard and soft acids and bases, HSAB, part 1: Fundamental principles, *Journal of Chemical Education*, 45, 9, (1968), 581
https://doi.org/10.1021/ed045p581

[23] P. W. Atkins, T. L. Rourke, J. P. Overton, M. T. Weller, F. A. Armstrong, *Inorganic Chemistry*, Oxford University Press, Oxford, 2010

[24] Ana Toyyibatun Nasukhah, Fabrikasi dan Karakterisasi Dye Sensitized Solar Cell (DSSC) dengan Menggunakan Ekstraksi Daging Buah Naga Merah (Hylocereus Polyrhizus) sebagai Dye Sensitizer, *undergraduate thesis*, Physics Department, Institut Teknologi Sepuluh Nopember, Surabaya, 2012

[25] Hadi Santoso, Vicran Zharvan, Rizqa Daniyati, Nur Ichzan Aminuddin Siantang, Gatut Yudoyono, Endarko Endarko, Peningkatan Kinerja Dye-Sensitized Solar Cells menggunakan Metode Ultrasonikasi, *Jurnal Fisika dan Aplikasinya*, 11, 1, (2015), 32-35
https://dx.doi.org/10.12962/j24604682.v11i1.783

[26] Anita Listanti, Ahmad Taufiq, Arif Hidayat, Sunaryono Sunaryono, Investigasi Struktur dan Energi Band Gap Partikel Nano $TiO_2$ Hasil Sintesis Menggunakan Metode Sol-Gel, *Journal of Physical Science and Engineering*, 3, 1, (2018), 8-15
https://doi.org/10.17977/um024v3i12018p008

[27] Akhiruddin Maddu, Mahfuddin Zuhri, Irmansyah Irmansyah, Penggunaan Ekstrak Antosianin Kol Merah sebagai Fotosensitizer pada Sel Surya $TiO_2$ Nanokristal Tersensitisasi Dye, *Makara Journal of Technology*, 11, 2, (20097), 78-84
https://doi.org/10.7454/mst.v11i2.529

[28] Yulia Nadhirah, RD Kusumanto, Abu Hasan, Increasing Efficiency of Dye-Sensitized Solar Cell (DSSC) Originating from Yellow Sweet Potato Extract as Dye Sensitizer: Effect of Acetic Acid, Polyethylene Glycol, and Polyvinyl Alcohol as $TiO_2$ binders, *Jurnal Kimia Sains dan Aplikasi*, 23, 11, (2020), 403-408
https://doi.org/10.14710/jksa.23.11.403-408

[29] Xiliang Nie, Shuping Zhuo, Gloria Maeng, Karl Sohlberg, Doping of $TiO_2$ Polymorphs for Altered Optical and Photocatalytic Properties, *International*

*Journal of Photoenergy*, 2009, (2009), 294042 https://doi.org/10.1155/2009/294042

[30] Saad Sh. Al-Omary, Laith A. Algharagholy, Mohsin E. Al-Dokheily, Band Gap Modification of $TiO_2$ Using Solid State Reaction with Hydrides in Argon Atmosphere, *International Journal of Engineering and Technology*, 7, 4, (2018), 354-362 https://doi.org/10.14419/ijet.v7i4.36.23804